Aeolian sediment in El Paso, Texas: Elevated desert sand deposition rates and dust concentrations, enhanced by drought and urban sources

Thomas E. Gill[1,*], Jose A. Rivas Jr.[2], and Elizabeth J. Walsh[2]

[1] Department of Earth, Environmental and Resource Sciences, University of Texas at El Paso, El Paso, TX 79968 USA

[2] Department of Biological Sciences, University of Texas at El Paso, El Paso, TX 79968 USA

* Corresponding author. Email: tegill@utep.edu

ORCID IDs:
Thomas E. Gill https://orcid.org/0000-0001-9011-4105
Jose A. Rivas Jr, https://orcid.org/0000-0003-2101-1115
Elizabeth J. Walsh https://orcid.org/0000-0002-6719-6883

Abstract

Deposition of aeolian (windblown) dust and sand in drylands, such as the El Paso, Texas, USA / Ciudad Juarez, Chihuahua, Mexico metropolitan area within the Chihuahuan Desert, impacts soils, ecosystems, human infrastructure, and air quality. We monitored dry bulk deposition using marble dust collectors (MDCOs), a passive sampler, deployed atop a university building 21m above ground level during synoptic-scale wind events in urban El Paso, for five years (2011-2016). A nearby Texas Commission on Environmental Quality air monitor continuously measured particulate matter concentrations. MDCO sediment deposition rates over five synoptic dust event seasons (October- May) averaged 111 $gm^{-2}yr^{-1}$ (range 85 – 164 $gm^{-2}yr^{-1}$), higher than almost all other North American sites but generally lower than Global Dust Belt locations. These deposition rate values, representing only synoptic-scale wind events, underestimate total annual aeolian deposition (augmented by convective dust events and inputs during non-windstorm conditions). Deposition rates were ~2x those reported for rural El Paso County, suggesting urban fugitive dust enhances total dry deposition. Mean grain size of deposited sediment in all events was >50 μm (sand), even though collected ~20 m above the height of saltation, indicating that events in El Paso can be considered "blowing sand" rather than "blowing dust." PM_{10} concentrations averaged 28 $\mu g/m^3$ over all collection years but 200 $\mu g/m^3$ during hours dust was observed, were extremely variable, and were significantly higher during years of strong drought. $PM_{2.5}/PM_{10}$ ratios averaged 0.13-0.14 during collection periods and dust hours. $PM_{2.5}$ concentrations were less strongly variable, showing the roles of dust and drought in PM_{coarse} in El Paso. Back trajectories during synoptic events were predominantly from the southwest and west, crossing sandy, erodible desert soils and remote-sensing-identified dust hotspots. MDCO sediments were comprised primarily of predominant Chihuahuan Desert soil minerals (quartz, feldspars, and calcite). Compared to global

average aeolian deposition of major and minor elements, El Paso samples were enriched in silicon but depleted in aluminum, titanium, and manganese, as well as iron, an element with important ecological, radiative, and human health impacts. El Paso, Texas appears to be one of the dustiest / sandiest cities in North America.

KEYWORDS: Urban atmospheric dust, aeolian sand, Chihuahuan Desert, particulate matter, particle size, HYSPLIT, marble dust collector

1. Introduction

Dry deposition of aeolian (windblown) dust and sand represents an important physical and chemical flux of matter and nutrients in and downwind of deserts (Prakash et al., 2016). Falling dust and sand has numerous environmental effects, affecting the composition and structure of dryland soils (Munroe et al., 2024; Rea et al., 2020; Reheis et al., 1995), impacting plant physiology (Jiao et al., 2018; Soheili et al., 2023), and altering snowpack composition and hydrology (Reynolds et al., 2014). Falling aeolian sediment impacts human infrastructure, soiling buildings and machines (Duniway et al., 2019), contaminating drinking water (Sanchez et al., 2015), reducing traction on paved roads (Pan et al., 2021), inhibiting the performance of photovoltaic systems (Abuzaid et al., 2022), and degrading overhead electric power lines (Maliszewski et al., 2012). Dust is a major component of airborne particulate matter in drylands and regions downwind of them, resulting in potentially hazardous concentrations of air pollution (Rivera Rivera et al., 2010).

An effective, low-tech, widely-used technique to collect and quantify windblown sediment is the deployment of passive collectors (dust traps). Marble dust collectors (MDCOs) (Goossens and Offer, 2000) have been frequently utilized to capture falling dust and sand and determine dust deposition rates (Sow et al. 2006). Advantages of MDCOs are that collected dust particles are protected against deflation by wind and rain, and help diminish bias in the particle size distribution of collected dust (Sow et al., 2006).

The largest metropolitan area in the Chihuahuan Desert of North America is El Paso, Texas, USA/ Ciudad Juarez, Chihuahua, Mexico (the Paso del Norte region), with a combined population of over 2 million. The city of El Paso, at the westernmost point of Texas, is separated from Ciudad Juarez by the Rio Grande/ *Rio Bravo Del Norte* river. There is a large residential and

industrial component of El Paso along with open desert and mountain topography contained within city limits. Air quality issues in the metropolitan area include excessive ozone (Karle et al., 2021), gaseous pollutants (McCoy et al., 2010), traffic-related emissions (Raysoni et al., 2011), industrial emissions (Grineski and Collins, 2010), and fugitive dust resuspended within the metropolitan area (Garcia et al., 2003, 2006). However, windblown desert dust represents the most frequent and most extreme threat to air quality in El Paso (Novlan et al., 2007: Rivera Rivera et al., 2010) (Figure 1).

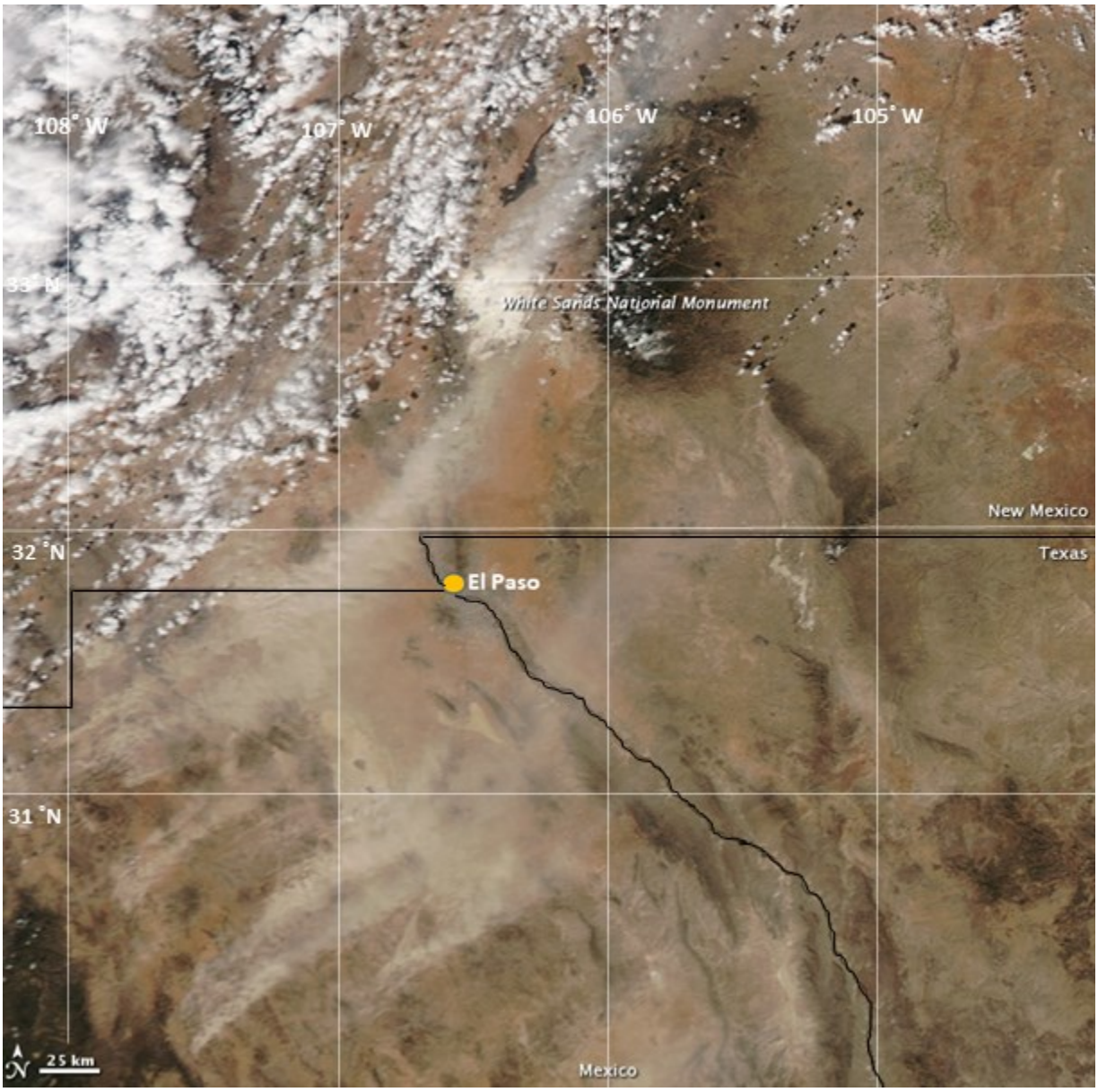

Figure 1. NASA MODIS Terra image of windblown dust/sand plumes approaching El Paso, Texas on February 20, 2013. Orange dot represents approximate location of sampling site. Image credit: Jeff Schmaltz, MODIS Land Rapid Response Team, NASA GSFC. Retrieved from https://earthobservatory.nasa.gov/images/80491/dust-storm-in-mexico-and-new-mexico .

Encompassing a climatic boundary between the subtropics and the middle latitudes (Castiglia and Fawcett, 2006), the northern Chihuahuan Desert experiences strong winds causing frequent dust events, forming one of the main dust sources in North America (Prospero et al.,

2002). El Paso averages approximately 22 dust events per year (Robinson and Ardon-Dryer, 2024). Dust and sand transport around El Paso causes exceedances of air quality standards (Lee et al., 2009; Rivera Rivera et al., 2010), deflates soil and leads to sand dune formation (Gillette and Monger, 2006; Langford, 2000), transports aquatic microinvertebrates to new habitats (Rivas et al., 2018, 2019), reduces visibility presenting a significant driving hazard (Li et al. 2018; Tong et al., 2023), and impacts human health (Grineski et al., 2011; Herrera-Molina et al., 2021; Tong et al., 2017). Dust generated in the Chihuahuan Desert near El Paso can cause transient spikes in particulate matter concentrations hundreds of kilometers downwind (Lee et al., 2009) and has been detected in wet deposition thousands of kilometers downwind, in southeastern Canada (Park et al., 2007).

Windblown dust and sand in the Chihuahuan Desert tends to occur as distinct types of events in different seasons. Synoptic events occur with west to southwest winds during the drier, cooler part of the year (October- May) (Novlan et al., 2007), typically associated with Pacific frontal passages and low-pressure areas traversing to the north (Rivera Rivera et al., 2009). Mesoscale events, typically convective outflows (haboobs) associated with the North American monsoon, primarily occur in June through August (Novlan et al., 2007). Source areas upwind of El Paso include playas (dry lake beds), dry riverbeds, and alluvial lowlands in the Chihuahuan Desert (Baddock et al., 2011, 2016, 2021), as well as agricultural lands in Chihuahua, Mexico (Lee et al., 2009; Rivera Rivera et al, 2010). Desert sand sheets surrounding El Paso (Langford, 2000) emit dust which impacts the city (Baddock et al., 2011), while gypsum dust from White Sands, New Mexico (White et al., 2015) occasionally advects into El Paso from the north-northeast. In the air quality management context, El Paso's dust events and the strong influence of regional transport pathways into the city represent "exceptional events" from natural sources and/or from

beyond international borders, which are not reasonably controllable or preventable (Dayalu et al., 2024). Within the metropolitan area, locally-generated fugitive dust emanates from unpaved roads, bare lots, construction sites, and industrial facilities (Garcia et al., 2003).

Aeolian dust/sand deposition has been measured elsewhere in west Texas, including Lubbock (Crabtree, 2004; Warn and Cox, 1951), Big Spring (Crabtree, 2004), Salt Flat Basin (Perez and Gill, 2009), and rural El Paso County (Ortiz and Jin, 2021; Rivas, 2019), but not within urban El Paso. Given that knowledge gap, the aim of this project was to determine deposition rates, particle size, elemental, and mineralogical composition of aeolian dust and sand being transported to the city of El Paso, Texas during synoptic-scale events, and place these properties in context to other dust-prone cities in North America and elsewhere. The samples used in this work were collected using MDCO passive deposition traps initially to investigate wind dispersal of aquatic microinvertebrates (Rivas et al. 2018, 2019). Rivas et al. (2018, 2019) include some event-specific data on amounts of sediment deposited from individual wind events along with selected HYSPLIT trajectory results showing regional dust source areas. This study aggregates more than five years of deposition data, alongside particulate matter concentration data from a nearby continuous air monitoring station, to quantify and characterize dry dust/sand deposition in El Paso.

2. Methods

Samples of the wind-deposited dust and sand from which microinvertebrate propagules were rehydrated by Rivas et al. (2018, 2019) were analyzed to determine dust deposition rates, particle sizes, and chemical and elemental composition. Wind trajectories from the events and measurements from an adjacent air monitoring station were used to contextualize transport

pathways and particulate concentrations associated with these dry deposition event characteristics. Some experimental methods pertinent to this study were summarized in Rivas et al. (2018). A full description of the methods is provided and expanded on here.

2.1 Sample Collection/Dust Deposition

Bulk falling aeolian sediment was collected with MDCOs on the flat rooftop of the Biology Building on the campus of the University of Texas at El Paso (UTEP) (31.768 N, –106.504 W; elevation 1170 m, height of 21 m above the ground), in an urbanized southwest part of the metropolitan area (~7 km downwind of the edge of open desert, but in the upwind part of the Paso del Norte metropolitan area for most events). Collections were made from March 2011- May 2016 and stopped in fall 2016 when major land clearance and construction activities commenced <150m away, exposing bare soil and causing fugitive dust to be emitted near the sampling site.

A total of 68 synoptic wind events were sampled on an event-by-event basis. Thirteen events were briefly described in Rivas et al. (2018) and meteorological, event-specific deposition, and PM data on 67 of the events were included in Supplemental Document 1 in Rivas et al. (2019). A collection season was defined as from October through May, as dust/sand events from June through September are almost exclusively mesoscale events associated with convective storms of the North American Monsoon (Novlan et al., 2007; Robinson and Ardon-Dryer, 2024), and only synoptic events with only dry deposition (no precipitation while traps were deployed) were sampled. Traps were not deployed for dust events when precipitation was also forecast due to the need for samples to remain dry for biological analyses (Rivas et al., 2018, 2019). Any unforecasted synoptic-scale blowing dust/sand events, all of short duration and intensity, were not sampled. When a forecasted event did not materialize, no detectable amounts of sample were deposited in

the MDCOs, and it was not counted as an event. Six samples from Spring 2011 are not included in collection year deposition rate data. $PM_{2.5}$ and PM_{10} data from the adjacent air quality monitoring site were not available during three events due to monitor malfunction or maintenance happening at those times. Only seven samples were collected during 2014–2015, primarily due to transport capacity limitation (lack of wind). For this reason, several samples representing long-term collection periods or background conditions were undertaken during this year, including stretches of multiple days (12/13/2014–2/15/2015) in which dust was not reported in airport weather observations.

MDCOs (traps) (n=7) with a total surface area of 0.9 m^2 were placed on the rooftop in scattered orientations the day before each forecasted dust event and were deployed until meteorological observations of dust at El Paso had concluded and continued dusty conditions were no longer forecasted. Events were forecasted by monitoring the United States National Weather Service- El Paso's twice-daily Area Forecast Discussions for mention of possible blowing dust or dust storm during the next day. Hourly or more frequent weather observations (including visibility, wind speed, wind direction, wind gust, event start time, and event end time) at El Paso International Airport, 10.6 km east of the dust sampling site, were collected, with airport weather observations of dust events (Blowing Dust, Dust, Dust Storm, or Haze with wind speed > 20 mph (8.9 m/s) and without precipitation; as reported by and with the criteria used by the USA National Weather Service (Ardon-Dryer et al., 2023)) noted.

Traps were also set out during a non-dusty wind event from 1/10/13 to 1/13/13 in which wind speeds were light to breezy and dust was not being forecast or suspended, to characterize local "background" deposition rates and characteristics outside of identified events. Average wind speed during this collection period was 2.6 m/s. During the October 2014- May 2015 synoptic dust

season El Paso experienced very few wind events, so traps were left out for longer periods of time, from weeks to months, and data from the 2014-2015 season includes a larger proportion of background conditions.

Sample collection procedures were adapted from Goossens and Rajot (2008). Using fine angled clean paintbrushes, one for each trap, the dust was brushed into a corner, placed into small clean containers and weighed with an analytical balance. Each sample was divided into up to four subsamples; the first for rehydration of biota (see Rivas et al., 2018, 2019), the second for particle size analysis, the third for mineral composition, and if sufficient sample remained, the fourth for elemental analysis. A minimum of 1.5 g of deposited sediment per event aggregated from all MDCOs was sufficient to run all four analyses. Deposition rate was calculated by dividing the total amount of material collected per event by the total surface area of all traps over the time MDCOs were deployed. Deposition rate over the synoptic dust season (October-May) was expressed as g/m^2/year, a convenient and widely-used metric for such studies (Lawrence and Neff, 2009).

2.2 Associated Particulate Matter Monitoring

A Texas Commission on Environmental Quality (TCEQ) continuous air monitoring station (CAMS-12) was located 217m east-southeast of the MDCO collection site. The CAMS continuously recorded hourly data on weather and air quality, including $PM_{2.5}$ and PM_{10} concentrations measured by tapered element oscillating microbalance (TEOM) (Ruppecht et al., 1992). Aerosol and meteorological data from the CAMS-12 site were obtained for each dust event.

2.3 Source area/trajectories

Transport pathways of dust associated with each of the 68 events were determined by creating back trajectories of wind arriving at UTEP: 13 of which were described in Rivas et al. (2018). Trajectories were calculated using the NOAA HYSPLIT model (Stein et al., 2015). Default parameters were used with a total run time of 24 hrs (or the duration of the dust event), number of trajectories set to 24, and a height of 500 m above ground level (representing dust in the boundary layer which therefore could be deposited) for each event. The ending time for each HYSPLIT run was the hour when PM_{10} concentration first decreased below 100 $\mu g/m^3$ at the TCEQ CAMS-12 site. The receptor site, UTEP, was selected by using the latitude and longitude coordinates of the traps.

2.4 Grain size determination

Approximately 0.3 g of sample per event was tested following general procedures for direct wet grain size analysis by laser diffraction (Sperazza et al., 2004), using a Malvern Mastersizer 2000 Laser Diffractometer (Malvern Instruments, Worcestershire, UK). To prepare the sample, the sediment was sieved to remove any grains >2 mm (larger than sand size), placed in a clean plastic bottle and 20 ml of sodium hexametaphosphate solution (50 g/L) was added. The mixture was then placed on a reciprocating shaker for at least 8 hr. After shaking the sample was then placed into the HydroG circulating fluid vessel of the Mastersizer and a standard operating protocol was initiated, including sonication of the sample for 60 seconds at 80% of full sonication. Obscuration of the sample during laser diffraction analysis was kept between 10 to 20 % to optimize sample analysis. The system was flushed with ultrapure distilled water before each analysis, and a test analysis was conducted prior to analyzing the dust sample using ISO standard

12103-1, A4 Coarse Test Dust (Powder Technology Incorporated, Arden Hills, MN, USA). Particle size classification scheme adapted from the USDA (Soil Survey Division Staff, 1993) was used to identify equivalent textural classes (sand, silt, clay) of each sample of wind-fallen sediment. Grain sizes were classified as clay (<2μm), silt (2 – 50μm), and sand (>50μm).

2.5 Mineral composition

If enough sample remained after particle sizing, approximately 0.25g was used for mineralogical characterization with a Rigaku Miniflex II Benchtop X-Ray Diffraction (XRD) instrument. Samples were prepared by pulverizing the material in a synthetic ruby mortar and pestle with 100% acetone until it obtained a fine consistency and a paste-like substance was formed. Jade 9.0 (Jade Software Corporation), DIFFRAC^{PLUS} Bruker AXS (1996-2007) (Bruker Instruments Inc.), and EVA 14.0 (Bruker Instruments Inc.) programs were used for pattern processing and identification of mineral phases. Clay mineral analyses were not performed.

2.6 Elemental analysis

If sufficient sample remained after XRD, elemental analysis for likely major and minor elements (Na, Mg, Al, Si, P, K, Ca, Ti, Mn, Fe, Sr, Zr, Ba) was performed using inductively-coupled plasma optical emission spectroscopy (ICP-OES, Perkin Elmer 5300 DV I). The lithium metaborate fusion technique (Feldman, 1983; Ingasmells. 1970; Medlin et al., 1969; Suhr and Ingasmells, 1966) was used for sample preparation. Approximately 0.1 g of sample was added to 1.0 g of lithium metaborate and shaken for 2 min. Samples were placed into a crucible and placed into an oven at 900°C for 15 min. Samples were then poured into Teflon beakers with 100 ml of 5% nitric acid and stirred for 15 min. Prior to analysis samples were diluted with 5% nitric acid at

a ratio of 1:10. The mixture was then transferred to polyethylene bottles until analysis by ICP-OES. Following the protocols of Nyachoti et al. (2019), twenty rock standards from NIST and USGS were digested and analyzed with each batch of samples using the same procedure and used as calibration standards for major elements along with a procedure blank, and the USGS reference rock material W-2 was digested and analyzed with each batch of samples as a quality check. The differences between measured and certified values in all major element concentrations on W-2 were < 10%. There was an apparent system error in elemental analyses of the 2014–2015 and 2015–2016 samples; data for these samples are not included.

2.7 Data Analysis

Several statistical techniques were used to analyze some of the datasets. One-way analysis of variance (ANOVA) was used to test for significant differences among annual average PM_{10} concentrations and texture of sediment deposited into the MDCOs. ANOVA tests were used to determine the differences among mean of PM_{10} concentrations for all sampling hours, collection hours, and dusty hours. SAS Proc GLM (SAS 9.4, 2019) and Duncan Multiple Comparison methods were used for the ANOVA with significance level for all analyses set at 0.05. Additionally, $PM_{2.5/10}$ ratios between MDCO and CAMS data were analyzed using SAS software version 9.4 (SAS Institute, Inc., 2019) as Two-Sample Independent Sample T- test. The assumption of equality of variances was checked using Levene's test (Zar, 2009) and then equal variances T-test (pooled) or unequal variances T-test (Satterthwaite T-Test) were used for PM_{10} and $PM_{2.5}$ yearly comparisons (Zar, 2009).

3. Results and Discussion

A total of 68 events were sampled. Six samples from Spring 2011 are not included in collection year deposition rate data since they represented only part of a collection year.

3.1 Deposition Rate

Summary data including number of events sampled, number of days traps were deployed, and sediment deposition rate for each year are shown in Table 1.

Table 1. Summary data for dust trap deployment and deposition rate over five consecutive collection seasons.*

Collection season (Oct-May)	Number of synoptic dust events sampled	Number of days MDCOs were deployed	Deposition rate, $g/m^2/yr$
2011-2012	11	66	104
2012-2013	16	47	164
2013-2014	13	80	101
2014-2015	7	181	85
2015-2016	15	70	103
Total	**62**	**444**	**Mean, SD: 111 ± 30**

***** Six events in Spring 2011 are not included as part of a collection season.

Annual deposition rates of falling dust and sand trapped atop the UTEP Biology Building during synoptic dust events over collection seasons ranged from 85 $g/m^2/yr$ to 164 $g/m^2/yr$ for the five-year period (Figure 2). Average annual deposition rate was 111 $g/m^2/yr$. The highest deposition rate occurred in 2012- 2013, the year with the greatest number of events, as well as the culmination of an extensive drought. The reduced rainfall over the Southwestern USA during prior seasons through 2011, intensifying into 2012, and ecosystem "memory" of soil moisture and drought resulted in increased dust emission in the Chihuahuan Desert (Eibedingil et al., 2024;

Hoerling et al., 2014). Conversely, during the 2014- 2015 collection season, less of the surrounding region was in drought (Eibedingil et al., 2024), and there were fewer wind events; the deposition rate was the lowest, suggesting that this season was somewhat transport capacity and/or sediment availability limited.

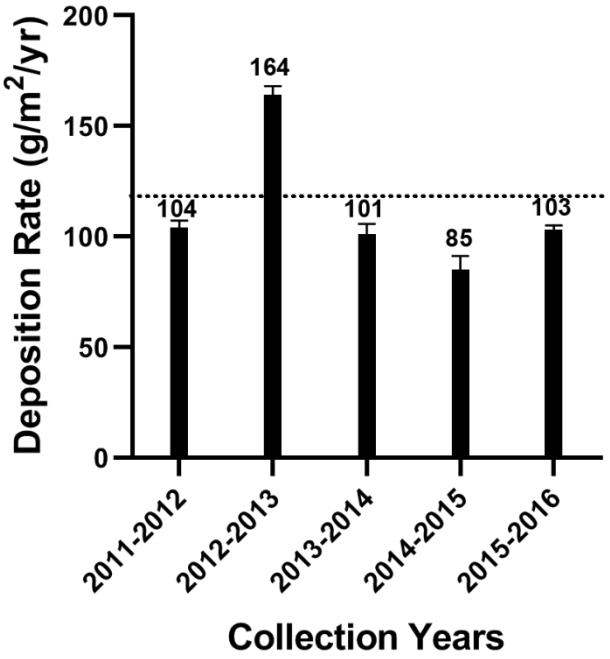

Figure 2. Yearly falling aeolian sediment deposition rates reconstructed from sampled synoptic dust events for 2011-2016 collection years at the UTEP Biology roof site. Dotted line represents five-year average of 111 g/m^2/yr. Error bars represent systematic error.

Deposition rates from passive aeolian sediment traps should be considered a general range best compared to other deposition measurements obtained with the same type of collector. With any kind of passive falling-sediment collector, deposition rates and characteristics such as particle size of material collected are dependent on factors including emission rate at the source (Shao, 2008), dust/sand concentration, wind velocity (Gong et al., 2024; Sow et al., 2006), orographic

features of the environment (Lawrence and Neff, 2009), wind gustiness (Yan et al., 2017), land use/ land cover changes (Belnap et al., 2009), and overall weather conditions throughout the source area (Reheis and Kihl, 1995). While MDCOs are widely used and their data are widely reported, the amount and characteristics of sediment they collect will depend on the specific design and dimensions of collector used (Gong et al., 2024; Goossens, 2007; Sow et al., 2006), orientation of the trap with regards to the wind direction (Sow et al., 2006), height above the land surface (Goossens and Rajot, 2008) and urban topography including location within the urban area and density and orientation of buildings (Erell and Tsoar, 1997; Putman et al., 2022). With these provisos in mind, Table 2 shows rates of aeolian sediment deposition obtained with marble dust collectors worldwide, including this study.

Table 2. Selected aeolian sediment deposition rates (dust + sand) from passive above-ground dust traps with marble substrate, including standard MDCO trap (Goossens and Offer, 2000) and USGS marble dust trap (Reheis and Kihl, 1995). Where four or more distinct sites were sampled, range and average are given if available.

Location	**Deposition rate ($g\ m^{-2}\ yr^{-1}$)**	**Source**
Kuwait City, Kuwait	340-940 Average: 590	Al-Awadhi and Al-Shuaibi (2013)
Riyadh, Saudi Arabia	454	Modaihsh et al. (2017)
Farmington Bay playa, Great Salt Lake, Utah	315- 404	Putman et al. (2023), Blakowski et al (2022, 2023)
Southern Owens Lake playa, California	~290	Reheis (2003)
Lake Qinghai, China	266	Wan et al. (2012)
Jabal Haroun, Jordan	≥250	Lucke et al. (2019)
El Paso-UTEP, El Paso County, Texas	111	This work
Lubbock, Texas	103	Crabtree (2004)
Big Spring, Texas	77	Crabtree (2004)
Beer Sheva, Israel (urban sites)	Long term: 49-95 Average: 74 single event: 1393	Erell and Tsoar (1997)

White Sands Missile Range, New Mexico	69	Velarde (2011)
Hueco Tanks State Park and Historic Site, El Paso County, Texas	56	Rivas (2019)
Northern Utah-urban regions	54	Scholz et al. (2019), quoted in Brahney (2019)
Southeast El Paso County, Texas	50	Ortiz and Jin (2021)
Salt Flat Basin, Texas	50	Perez and Gill (2009)
Northern Utah, 2022- excluding playa sites	16-74 Average: 35	Blakowski et al. (2023)
Northern Utah-urban regions	25-35 Average: 31	Goodman et al. (2019)
Northern Utah, 2018- 2019, urban regions	8-82 Average: 24	Blakowski et al. (2022)
Rio Grande Valley, southern New Mexico	10-60 Average: 23	Gile and Grossman (1979)
Colorado Plateau, Utah	14-32 Average: 22	Belnap et al. (2009)
Canyonlands region, Utah, 1999- 2008 (average of multiple sites)	22	Reheis and Urban (2011)
Southern Nevada, Southern California, 1984-1999	8-207 Average: 18	Reheis (2003)
Southern Sierra Nevada, California	6-36 Average: 16	Aciego et al. (2017)
Northern Sacramento Mountains, New Mexico	11	Rea et al. (2020)
Mojave Desert and Southern Great Basin, 1999- 2008 (average of multiple sites)	9	Reheis and Urban (2011)
Perry Mesa, Yavapai County, northern Arizona	3-14	Nakase et al. (2014)
Front Range, Colorado	5	Ley et al. (2004)

Although the MDCO dust and sand deposition rate in urban El Paso is lower than those of most sites in the "global dust belt" (region defined by Prospero et al., 2002), it is higher than rates reported elsewhere in North America, except for at the downwind edges of dust-emitting playas including Owens Lake (Reheis, 2003), which has been one of the continent's most intense dust sources (Cahill et al., 1996; Reheis, 2003), and the Farmington Bay playa of Great Salt Lake, an

intensifying dust source (Blakowski et al., 2022, 2023; Putman et al., 2023). Bulk deposition rates are relatively higher in the eastern Chihuahuan Desert sites (El Paso, White Sands Missile Range, Hueco Tanks State Park and Historic Site, Southeast El Paso County, Salt Flat Basin) extending into the Southern High Plains (Lubbock, Big Spring) than reported for the rest of North America (Table 2). This region also broadly matches a springtime (synoptic dust season) zone of enhanced coarse aerosol mass ($CM = PM_{10} - PM_{2.5}$) consistent with synoptic-scale airflow patterns (Hand et al., 2019). Deposition rates in the urbanized Wasatch Front of Utah are slightly lower than in the Chihuahuan Desert but slightly higher than those reported for the interior mountains and Colorado Plateau. The Mojave Desert and southern Great Basin appear to have lower deposition rates of falling dust and sand than other USA drylands. High-elevation sites (northern Sacramento Mountains, Front Range) have low vertical flux of aeolian sediment, much as they have reduced CM due to increased land cover, distance from dust sources, less bare soil, and/or elevation-limited transport (Hand et al., 2019). No MDCO measurements appear to have been reported from some other dusty regions, such as the Sahara and Sahel of Africa, the Aral Sea basin, or the Sonoran Desert lowlands and Columbia Plateau of the United States, so data from those areas are not included in Table 2.

Table 1 and Figure 1 in Lawrence and Neff (2009) show a comprehensive list of annual deposition rates from 52 sites worldwide ranging from 0.05 $g/m^2/yr$ at Penny Ice Cap, Canada (representing minimum global background transport) to 450 $g/m^2/yr$ (local transport) in China. Compared to Lawrence and Neff (2009)'s findings, El Paso-UTEP average annual deposition would place above the 80^{th} percentile of the reported areas. Figure 3 shows El Paso- UTEP data in the context of their results. By Lawrence and Neff (2009)'s classifications, El Paso- UTEP dust would be considered "local," very near to active source areas, having travelled ~10km or less from

the source. While most of the dust sources identified by remote sensing as impacting El Paso (Baddock et al., 2011, 2021; Rivera Rivera et al., 2010) would be considered "regional" in nature (~100 km upwind) and expected to be associated with lower deposition fluxes, the deposition rates measured at UTEP were approximately twice those measured in rural portions of El Paso County (Ortiz and Jin, 2021; Rivas, 2019) (also shown on Figure 3), suggesting urban enhancement of deposition rates. There are a wide variety of fugitive dust sources throughout the Paso del Norte metropolitan area (Garcia et al., 2003), and the MDCO deployment site is <1 km downwind of Ciudad Juarez, Mexico, a city with a high percentage of roads that are unpaved and highly fugitive-dust-emissive (Kavouras et al., 2016). The high rate of dust and sand deposition at the UTEP- El Paso site is consistent with increased dust deposition rates in urban areas, due to local anthropogenic dust sources (Sorooshian et al., 2011), as well as deceleration of particle-laden winds as they enter a roughness-enhanced urban area which causes dust deposition (Zhang et al., 2001; Putman et al., 2022).

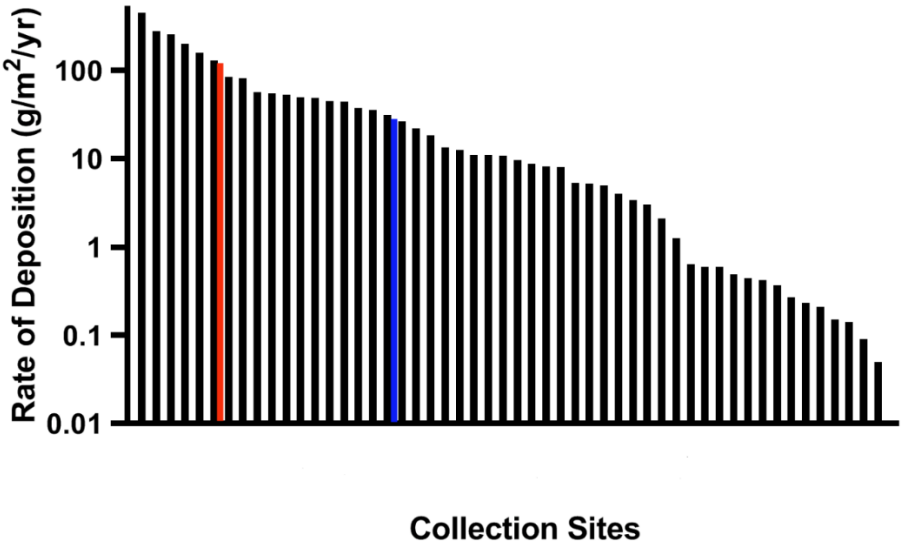

Figure 3. Rank ordered rates of dust deposition from 54 collection sites around the world, adapted from Lawrence and Neff (2009). Deposition rates ranged from 0.05 g/m^2/yr to 450 g/m^2/yr. The red bar shows the average deposition rate (111 g/m^2/yr) for the UTEP collection site: the blue bar shows average deposition rates (53 g/m^2/yr) for rural sites in El Paso County (Ortiz and Jin, 2021; Rivas, 2019), suggesting urban enhancement.

On the other hand, the annual sediment deposition rates calculated for UTEP- El Paso must be underestimates, perhaps large ones. Due to the original purpose of the sampling (the collection of dry microinvertebrate propagules; Rivas et al., 2018, 2019), sediment traps were not deployed for synoptic events when precipitation was forecasted, nor for any convective dust events which are almost always accompanied by thunderstorms. Thus, multiple events were not sampled each year. In addition, a certain amount of background deposition takes place over the majority of the year outside of high-wind storm events.

3.2 Trajectories

HYSPLIT back trajectories associated with collected samples are shown in Figure 4, corresponding to synoptic-scale dry deposition events only and excluding the long term or "background" sample. A total of 67 trajectories were run, 13 of which were described in Rivas et al. (2018); trajectory results indicate airflow primarily from the westerly to southwesterly direction with several events originating from the northerly or easterly directions. The dominant transport direction during synoptic dust events was from the southwest (57% of the trajectories), in accordance with the long-term record of prevailing dust-raising winds impacting El Paso (Novlan et al., 2007) and consistent with the direction of trajectories associated with anomalously high $PM_{2.5}$ concentrations in El Paso (Dayalu et al., 2024). An additional 22% of the trajectories came from the west, 7% from the south, 6% from the northwest and 3% from the southeast, 3% from the north and 2% from the northeast. The few trajectories from the north and northeast suggested

dust advecting to El Paso from the White Sands of New Mexico (White et al., 2015) and the Great Plains (Stout, 2001).

The surface horizons of soils underlying the trajectories west of El Paso on the U.S. side of the international border are generally mapped as loamy fine sands including poorly-developed soils developed from wind-blown sands (Soil Survey Staff, 2024) with ecological site descriptions of “sandy” and “deep sand” (Bestelmeyer et al., 2016). Trajectories arriving from Mexico cross soils mapped (using the International Union of Soil Sciences (2022) system) as calcic and eutric regosols in desert plains, and solonchak/solonetz in paleolake basins and alluvial lowlands (Instituto Nacional de Estadística, Geografía e Informática, n.d.). To summarize, trajectories arriving from the west and southwest over the Chihuahuan Desert (approx. 80% of trajectories during synoptic dust events) traverse erodible sandy and lacustrine soils that would readily entrain materials with compositions consistent with the subsequent mineral and elemental analysis. Remote sensing studies have identified multiple hotspots of dust emission within the southwestern and western transport pathways into El Paso, including alluvial lowlands of the Casas Grandes River (Rivera Rivera et al., 2010) and Mimbres River (Kandakji et al., 2020), playas such as the Paleolake Palomas Basin (Baddock et al., 2011, 2016, 2021), and sand sheets and dunes surrounding El Paso (Langford, 2000).

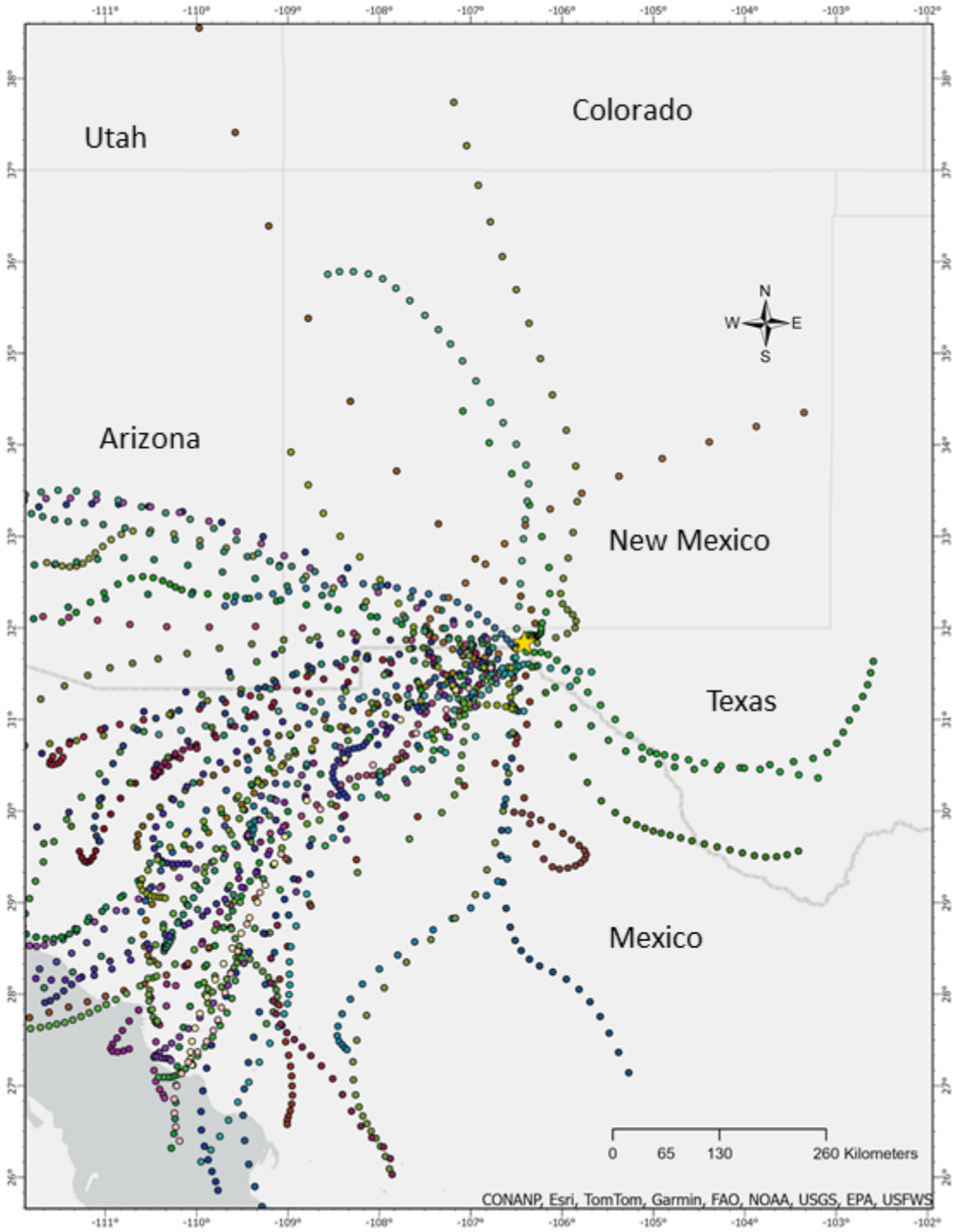

Figure 4. HYSPLIT 24-hour back trajectories for each of 67 dust events (the long- term sampled background event of 12/13/14 to 2/15/15 not included) over the five-year collection period, ending at the collection site in El Paso (yellow star).

3.3 Grain size and aerosol concentrations

A total of 54 events yielded sufficient sample to perform grain size analysis, 10 of which were reported in Rivas et al. (2018). Table 3 shows mean grain size of wind-carried sediments deposited in the MDCOs, $PM_{2.5}/PM_{10}$ ratios for those sediments, and corresponding $PM_{2.5}/PM_{10}$ ratios from the CAMS-12 TEOM. Table 4 shows the proportion of clay, silt, and sand sized grains in the MDCO-deposited sediment by collection year. Figure 5 shows grain size curves for MDCO data for each collection year.

Tables 5A and 5B show mean and peak hourly PM_{10} and $PM_{2.5}$ concentrations at the CAMS-12 site for each collection year and the five-year collection period for all hours; collection hours (all hours in which MDCOs were deployed); and dust hours (all hours in which dust was reported by weather observers at El Paso International Airport). Table 6 shows mean peak hourly PM_{10} and $PM_{2.5}$ concentrations per event at CAMS-12 for each collection year and the five- year sampling period.

Table 3. Grain size (mean ± SD) of sediments trapped in the MDCOs for each collection year and entire collection period. Proportion of particles in the MDCOs in PM_{10} and $PM_{2.5}$ size ranges and simultaneous $PM_{2.5/10}$ ratios for MDCO sediments and measured by CAMS-12 TEOM for collection hours also shown.

Collection year	Mean MDCO grain size (μm)	% PM_{10} MDCO (Mean ± SD)	% $PM_{2.5}$ MDCO (Mean ± SD)	$PM_{2.5/10}$ Ratio MDCO (Mean ± SD)	$PM_{2.5/10}$ Ratio TEOM (Mean ± SD)
2011–2012	106 ± 6.15	10.2 ± 5.47	4.12 ± 2.50	0.403 ± 0.05	0.13 ± 0.05
2012–2013	124 ± 5.26	9.50 ± 4.78	3.76 ± 1.66	0.395 ± 0.04	0.19 ± 0.08
2013–2014	99 ± 5.47	11.30 ± 5.76	4.12 ± 1.59	0.365 ± 0.05	0.13 ± 0.03
2014–2015	156 ± 4.68	6.20 ± 3.07	2.00 ± 0.67	0.323 ± 0.06	0.22 ± 0.09
2015–2016	122 ± 4.52	8.20 ± 4.80	3.02 ± 1.58	0.366 ± 0.05	0.17 ± 0.03
Entire period	108 ± 5.28	9.30 ± 4.15	3.50 ± 1.85	0.376 ± 0.05	0.14 ± 0.06

Table 4. Mean percent clay, silt, and sand of sediment trapped in the MDCOs for each collection year and for the entire collection period.

Collection Year	% clay	% silt	% sand
2011–2012	4.0 ± 2.3	21.0 ± 8.1	75.0 ± 10.0
2012–2013	3.2 ± 1.7	19.2 ± 6.1	77.6 ± 7.6
2013–2014	3.7 ± 1.4	22.7 ± 4.3	73.6 ± 5.1
2014–2015	1.7 ± 0.5	20.8 ± 7.5	77.5 ± 7.9
2015–2016	2.7 ± 1.5	19.2 ± 8.6	78.1 ± 9.8
Entire period (Mean ± SD)	3.17±1.75	20.02±7.08	76.79±8.46

Table 5A. Mean PM_{10} concentrations from TEOM data at CAMS-12 site by collection year for all hours, collection (MDCOs deployed) hours, and dust hours (as per weather observations at El Paso International Airport). Concentrations are given in $\mu g/m^3$, mean ± SD.

Collection year	PM_{10}, All hours	PM_{10}, Collection hours	PM_{10}, Dust hours	Peak hourly PM_{10}
2011–2012	31.0 ± 76.1^{a}	67.2 ± 212.2^{ab}	278.9 ± 528.1^{a}	4739
2012–2013	31.5 ± 59.4^{a}	66.6 ± 143.3^{a}	242.9 ± 281.2^{a}	1955
2013–2014	27.3 ± 47.7^{b}	68.7 ± 47.7^{a}	194.7 ± 225.0^{a}	1467
2014–2015	22.2 ± 20.7^{c}	25.2 ± 20.5^{c}	51.9 ± 47.5^{b}	281
2015–2016	28.7 ± 34.7^{b}	52.0 ± 107.8^{b}	116.9 ± 107.8^{b}	608
Entire collection period	27.9 ± 53.9^{c}	56.0 ± 140.1	200.2 ± 315.9	4739

Letters in each column indicate significant differences (ANOVA, Tukey range test, $P<0.05$)

Table 5B. Mean $PM_{2.5}$ concentrations from TEOM data at CAMS-12 site by collection year for all hours, collection (MDCOs deployed) hours, and dust hours (as per weather observations at El Paso International Airport). Concentrations are given in $\mu g/m^3$, mean ± SD.

Collection year	$PM_{2.5}$, All hours	$PM_{2.5}$, Collection hours	$PM_{2.5}$, Dust hours	Peak hourly $PM_{2.5}$
2011–2012	7.2 ± 7.9^{c}	9.0 ± 15.2^{b}	27.4 ± 47.2^{a}	414.2
2012–2013	8.0 ± 9.8^{c}	12.6 ± 21.6^{b}	37.2 ± 39.5^{a}	288.3
2013–2014	6.9 ± 7.5^{c}	9.0 ± 11.7^{b}	29.3 ± 31.5^{a}	195.2
2014–2015	6.1 ± 4.7^{b}	5.5 ± 5.0^{c}	9.0 ± 5.5^{a}	37.1
2015–2016	7.8 ± 7.1^{c}	8.7 ± 8.0^{b}	19.7 ± 15.5^{a}	97.1
Entire collection period	7.2 ± 7.6^{c}	7.8 ± 11.3^{b}	26.3 ± 33.3^{a}	414.2

Letters in each column indicate significant differences (ANOVA, Tukey range test, $P<0.05$)

Table 6. Peak hourly PM_{10} and $PM_{2.5}$ per event from TEOM data at CAMS-12 site averaged over all events for each collection year and entire collection period. Concentrations are given in µg/m^3, mean ± SD.

Collection Year	Average Peak Hourly PM_{10} Per Event	Average Peak Hourly $PM_{2.5}$ Per Event
2011–2012	1204.5 ± 1506	93.5 ± 134.2
2012–2013	723.2 ± 544.5	95.0 ± 75.2
2013–2014	523.8 ± 418.5	62.1 ± 59.0
2014–2015	156.8 ± 62.6	28.7 ± 16.0
2015–2016	287.0 ± 133.2	39.7 ± 22.5
Entire collection period	556.8 ± 707.1	66.3 ± 72

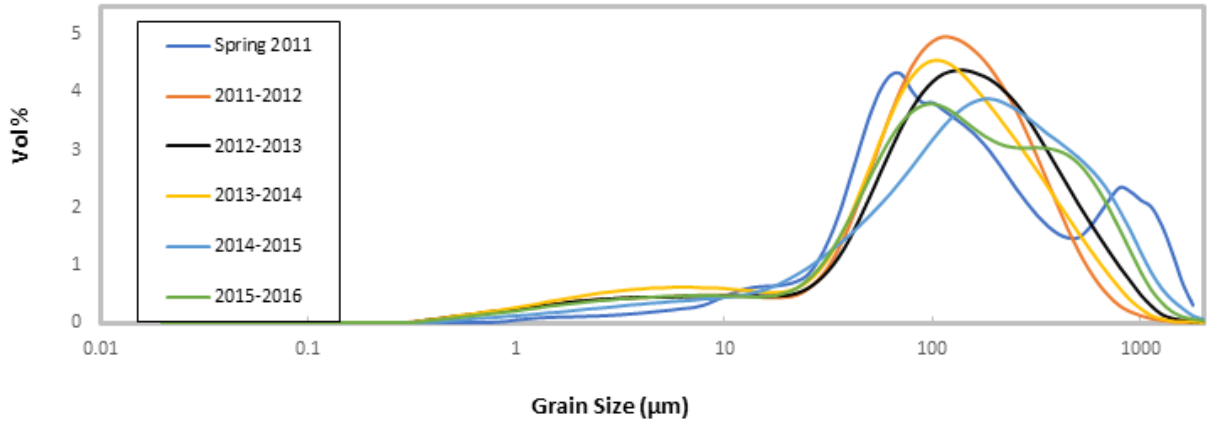

Figure 5. Grain size (via laser diffraction) of sediment collected from MDCO at UTEP Biology Rooftop, El Paso, Texas, by collection year.

Mean grain size of MDCO-deposited sediment in all events was greater than 50 µm, the boundary between silt (dust) and sand, even though collectors were deployed 21 meters above ground level. It is commonly assumed that suspension of sand-size particles is unusual and that most sand transport occurs as saltation (summarized in Zhang et al., 2021), though the height of the collectors was roughly an order of magnitude higher than the maximum height that sand grains generally move in saltation (Fryberger et al., 1979). Analysis of mean grain size of deposited sediment by collection year indicated that 2011–2012 (historic drought year) and 2014–2015 (low

wind and dust) collection periods were significantly different from the rest of the years. Annual average mean grain sizes for all years (Table 3) would be classified as fine or very fine sand, and based on clay, silt, and sand percentages (Table 4), the material deposited in the MDCOs for every collection year as well as the overall period would have a loamy sand texture (Soil Survey Division Staff, 1993). Mean grain size by event ranged from 56 μm (3/6–3/8/12) to 371 μm (1/23–1/26/16). These results are consistent with grain sizes of sand sheet and nabkha dune sediments surrounding El Paso (Langford, 2000), and the surface textures of wind-erodible soils in the Chihuahuan Desert lowlands to the west (Soil Survey Staff, 2024). Therefore, at least as collected at UTEP, since most of the grains in wind events are sand falling from suspension, these events in El Paso could be characterized as blowing sand or sandstorms, rather than blowing dust or dust storms. A sample of falling aeolian sediment in the Texas Panhandle from the 1930s "Dust Bowl" was also comprised predominantly of sand-sized particles (Gill et al., 2000). Deposition over five to six years in the Southern High Plains dust source region of Texas was evaluated by Crabtree (2004): MDCO samples collected in Big Spring were predominantly sand, while samples from Lubbock were predominantly silt.

El Paso has some of the highest average PM_{10} concentrations in the USA. In a study of average annual $PM_{2.5}$ and PM_{10} concentrations across the United States (Li et al., 2013), two sites in El Paso were the only locations with PM_{10} exceeding 40 $\mu g/m^3$. Values for CAMS-12 for our five-year collection period overall were not so high (28 $\mu g/m^3$), but during hours when dust was reported at El Paso International Airport, PM_{10} averaged 200 $\mu g/m^3$. PM_{10} concentrations during all hours, dust hours, and peak concentration per event were highest in the historic drought period of 2011- 2013, showing its influence on local aerosol concentrations. For all years except 2014-2015 (a period of low wind and dust), the standard deviation of PM_{10} concentrations exceeded the

mean value, illustrating the extreme variability of particulate matter concentrations in El Paso as driven by dust events. These relationships were not so clear-cut for $PM_{2.5}$, and ANOVA analyses indicated significant differences between mean PM_{10} concentrations and mean $PM_{2.5}$ concentrations per collection year, suggesting windblown dust's primary effect in El Paso is on PM_{coarse} (particles between 2.5 µm and 10 µm in mean aerodynamic diameter) concentrations. The mean peak hourly PM_{10} concentration over more than five years of synoptic-scale dust events in El Paso exceeded 550 $\mu g/m^3$ and the mean peak hourly $PM_{2.5}$ concentration during such events exceeded 65 $\mu g/m^3$, with large standard deviations. All numeric PM values should be considered general upper bounds due to TEOM PM concentrations being higher than those obtained with other samplers during high winds (Sharratt and Pi, 2018) and heavy dust conditions (Ono et al., 2000).

At the scale of an individual windstorm, the dust concentration (represented by peak hourly PM_{10}) will be related to sediment availability (the amount of material available to be eroded from the land surface, highly responsive to moisture levels and land cover) and transport capacity (the velocity of the wind) (Mockford et al, 2018). The greatest peak PM_{10} concentrations for individual events (Tables 5A and 6) occurred in 2011- 2012, the height of one of the most extreme drought periods of record in the region (Hoerling et al., 2014), which reduced regional land cover, temporarily increasing sediment availability and dust emission (Eibedingil et al., 2024; Munson et al., 2011; White et al., 2015). As drought conditions diminished in the Chihuahuan Desert and land cover recovered over the following years, dust emissions decreased (Eibedingil et al., 2024) and so did peak event PM_{10} concentrations at the El Paso receptor site (Tables 5A and 6). Peak event PM_{10} concentrations dropped to approximately an order of magnitude lower in 2014- 2015, the year of fewest events and ~40% lower total deposition, than during 2011- 2013. Note,

however, that total deposition was highest in 2012- 2013, when there was a greater total number of synoptic wind events (see section 3.1). Total deposition of falling aeolian sediment does not seem to be related to short-term PM_{10} concentration.

The mean $PM_{2.5}/PM_{10}$ ratio from CAMS-12 TEOM measurements during all collection periods was 0.14 (annual range 0.13 - 0.22) and during synoptic dust event hours was 0.13 (annual range 0.10-0.17, individual event range 0.06 - 0.36). This very low $PM_{2.5}/PM_{10}$ ratio in El Paso is consistent with high amounts of PM_{coarse} being dispersed by windblown dust and fugitive dust. It is broadly equivalent to the $PM_{2.5}/PM_{10}$ ratio during synoptic dust events at CAMS-12 for 2001-2010 (0.14) (Rivera Rivera, 2012), and consistent with ratios of 0.12 (measured with TEOM) during a windblown dust event in urban Spokane, Washington (Haller et al., 1999), 0.15 during a synoptic dust event in Lubbock, Texas (Ardon-Dryer et al., 2022), and ratios of ~0.07 to ~0.2 during high-dust periods in Phoenix, Arizona (Huang et al., 2015). $PM_{2.5}/PM_{10}$ ratio collection year averages for MCDO samples ranged from 0.32 to 0.40, with ratios for individual events ranging from 0.25 to 0.46. MDCO $PM_{2.5}/PM_{10}$ ratios were significantly larger than TEOM $PM_{2.5}/PM_{10}$ ratios for all collection years and the entire collection period (two-sample independent sample T-test, pooled method for all periods except for 2012-2013 (Satterthwaite method), with $P < 0.05$). MDCO PM ratios are much larger due to the sample preparation which breaks down compound grains (aggregates) into their component particles in a detergent solution, as well as the different sampling methodologies of the two devices. TEOMs tend to overestimate PM_{10} concentrations during conditions of high wind and/or dust (Sharratt and Pi, 2018), while MDCOs have many issues including decrease of efficiency as wind speed and particle size increase (Sow et al., 2006).

3.4 Mineral and Elemental Composition

Measuring the mineralogy and chemistry of aeolian dust and sand deposition not only helps understand its role in nutrient delivery to ecosystems, but also helps in understanding the geochemical flux from aeolian transport (Lawrence and Neff, 2009). XRD analysis results for MDCO-collected sediment from 46 events (Figure 6) indicated that quartz was the dominant mineral, present in all samples analyzed. In addition to quartz, measurable amounts of anorthite (37% of samples), albite (22% of samples), calcite (22% of samples), and microcline (17% of samples) were identified from samples. Gypsum, orthoclase, and muscovite were present in only a few samples.

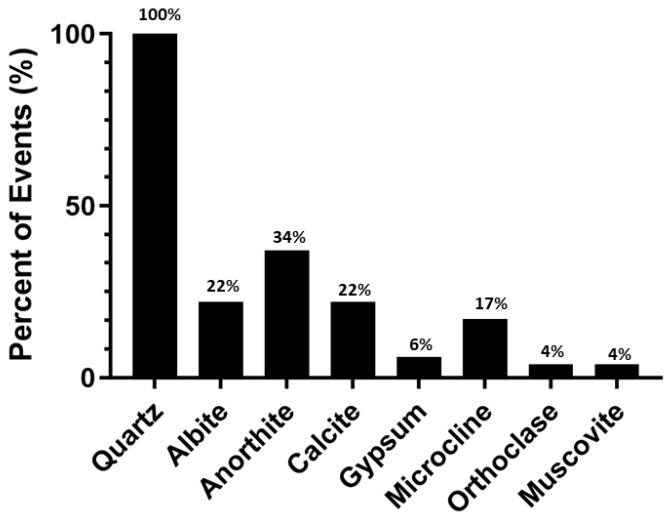

Figure 6. Mineral composition of 46 analyzed MDCO event samples for 2011–2016, expressed as percentage of all samples that each mineral was detected.

XRD results indicate aeolian deposition at UTEP is comprised of minerals found in wind-erodible soils of the Chihuahuan Desert (Peinado et al., 2014), as well as northern Chihuahuan

Desert soils in general (Gile et al., 1981) and dune sands immediately to the SW (upwind) of El Paso (Langford, 2000); quartz, feldspars, and calcite, with occasional presence of gypsum and micas. Clay minerals were not analyzed for in this study, though the MDCO samples likely contain clays. Aeolian sediment composition in El Paso is consistent with the mineralogy of locally-derived dusts worldwide (Lawrence and Neff, 2009). Quartz is the dominant mineral and silicon the dominant element in dusts, sands and soils from arid regions globally (Lawrence and Neff, 2009; Rashki et al., 2013), and these data show El Paso is no exception. Calcite likely occurs as fragments of pedogenic carbonate (caliche) which are present in local surface sands (Instituto Nacional de Estadística, Geografía e Informática, n.d.; Langford, 2000). Dust deposition is the major source of calcium for the formation of pedogenic carbonate in local desert soils (Capo and Chadwick, 1999; Ortiz and Jin, 2021), thus some of this calcium carbonate formed from dust is apparently cycled back into the atmosphere in local windstorms.

Elemental concentrations from ICP-OES analyses of 33 samples, presented as oxide equivalents, are shown in Table 7. Data show large amounts of Si (63% to 98% oxide equivalent, mean 76.3%, standard deviation 10.2%) reflecting the dominance of quartz and silicate minerals throughout all samples collected at UTEP. More than 10% Al as Al_2O_3 oxide equivalent, likely from feldspars and clay minerals, was detected along with 5% CaO likely from calcite, clay minerals, and feldspars. Minor amounts of Fe_2O_3, K_2O, Na_2O, MgO, TiO_2, P_2O_5 and MnO, were also detected, along with trace amounts (<1000 ppm) of Sr, Ba, and Zr.

Table 7. Elemental concentrations of El Paso MDCO samples obtained by ICP-OES (n=33), in bold, and estimated global means for deposited aeolian sediment from Lawrence et al. (2009). Concentrations represented in weight percentages as oxide norms or parts per million (ppm). Minimum (Min) and maximum (Max) indicate the range of each analyte detected in the samples. SD = standard deviation.

Element (Oxide norm)	Min %	Max %	Mean ± SD %	Estimated Global Mean (Lawrence et al., 2009)
SiO_2 %	**63.2**	**98.0**	**76.3 ± 10.2**	61.0 ± 1.7
Al_2O_3 %	**8.1**	**14.2**	**10.2 ± 1.4**	13.5 ± 1.3
CaO %	**2.7**	**8.4**	**5.0 ± 1.5**	5.0 ± 1.1
Fe_2O_3 %	**1.5**	**5.4**	**2.8 ± 0.8**	5.1 ± .6
K_2O %	**2.2**	**4.0**	**2.8 ± 0.58**	2.8 ± .2
Na_2O %	**1.0**	**3.2**	**1.9 ± 0.75**	1.6 ± .3
MgO %	**0.32**	**1.9**	**1.1 ± 0.5**	2.0 ± .9
TiO_2 %	**0.0**	**0.73**	**0.43 ± 0.16**	0.8 ± .2
P_2O_5 %	**0.0**	**0.50**	**0.18 ± 0.13**	0.25 ± .03
MnO %	**0.0**	**0.10**	**0.05 ± 0.02**	0.08 ± .01
Ba (ppm)	**622.0**	**1698.7**	**934 ± 304.7**	NA
Sr (ppm)	**282.5**	**590.8**	**380.3 ± 75.0**	NA
Zr (ppm)	**128.3**	**448.4**	**275.7 ± 74.2**	NA

ICP-OES analyses indicated elements associated with rock-forming minerals predominated in fallen dust and sand (e.g., Si, Al, Ca, Fe, Na, and K), consistent with the XRD results. Compared to averages for global aeolian deposition from Lawrence and Neff (2009), El Paso's samples are higher in Si and lower in Al, Fe, Ti, and Mn. Concentrations of Si in the MDCO samples are consistent with Si content of regional nebkha and sheet sands (Dominguez Acosta et al., 2010). Concentrations of Na, Mg, Al, K, Ca, Ti and Fe are slightly enriched compared to the composition of dune sands within the predominant wind transport pathway from the southwest into El Paso (Dominguez Acosta et al., 2010), while concentrations of Na, Mg, Al, Ti, Mn and Fe are slightly depleted compared to playa "dust hotspot" sediments along the same dominant transport path (Dominguez Acosta et al., 2007). The overall elemental composition of bulk aeolian sediments falling at UTEP suggests a dominant contribution from local sands, representing "quartz dilution," the outsized impact of larger particles on bulk sediment chemistry (Putman et al., 2022), with a subsidiary contribution from regional playa and alluvial dust sources.

Chihuahuan Desert dust tends to have a whitish to grayish appearance (Figure 7), lighter in color than dust from other North American dryland regions, likely due to its lower Fe and Mn content.

Figure 7. Light-colored windblown dust and sand shrouding the Anapra neighborhood of Ciudad Juarez, Chihuahua, Mexico, <2 km upwind of the MDCO sampling site.

The relative iron content is a key characteristic of dust from different source regions, due to the ecological, radiative, and human health impacts of iron in atmospheric particles (Al-Abadleh et al., 2023). Dust in the Southern High Plains tends to be reddish (Park et al., 2007) due to its high Fe content, where Fe/Si ratios in total suspended particulate samples in Lubbock approach 0.2 (Gill et al., 2009). Elsewhere, MDCO deposition in northern Arizona averaged 2.9%

elemental Fe (Nakase et al., 2014), slightly depleted from global averages, while iron content in windblown sediment fallout on a roof in the Phoenix, Arizona metropolitan area averaged 3.3% (Pewe et al., 1981) and dust trap samples in southern Nevada and southern California averaged approximately 3.5% Fe, very close to the global mean (Reheis et al., 2009). Silt-dominated aeolian deposition into the snowpack of the San Juan Mountains, Colorado, likely originating from the Colorado Plateau, averaged 2.4% Fe (Reynolds et al., 2020), and silt-dominated dust from the Great Basin deposited in snow of the Wasatch Range, Utah, during the April 14-15 dust storm in northern Utah averaged 2.3% Fe (Nicoll et al., 2020), lower than global averages. In comparison, iron content in aeolian deposition measured in El Paso averages lower than that from the aforementioned North American sites.

4. Conclusions

More than five years of data from passive aeolian deposition traps revealed the characteristics of falling dust and sand during synoptic-scale wind events in urban El Paso, Texas. Deposition rates were higher than reported for similar collectors in almost all other locations in North America, including surrounding rural sites in the Chihuahuan Desert, but lower than values reported for sites in the Global Dust Belt. Aeolian sediment deposition rates and PM_{10} concentrations at an adjacent air monitoring site were highest during a strong drought period, further suggesting the land-atmosphere feedback between drought and dust in the Chihuahuan Desert. The reported rates are underestimates of actual annual deposition, since samples were not obtained during convective dust events (haboobs) or most background (non-dust event) conditions.

El Paso, Texas appears to be one of the dustiest and sandiest cities in North America. The high deposition rates in El Paso may be due to (1) its location near and downwind of major

Chihuahuan Desert dust sources, as indicated by back trajectories and remote sensing; and (2) enhancement of dustfall in the urban area due to local sources of fugitive dust and urban topography which enhances deposition. Windstorms advect into El Paso primarily from the southwest and west, crossing erodible sandy soils and numerous dust emission hotspots in the northern Chihuahuan Desert across the international border. Analyses show that the aeolian sediment falling on El Paso, Texas is (1) primarily sand, not dust, such that events could be characterized as sandstorms, not dust storms, even though the collectors in this study were deployed 21 meters above ground level, well above the height of saltation; and is (2) similar in mineralogy (dominated by quartz, feldspars, calcite), and (3) broadly similar in major and minor element concentrations to other global dust-producing regions, though depleted in iron.

It has been established that dust events in El Paso are associated with increased hospitalizations for many conditions (Herrera-Molina et al., 2021), especially respiratory diseases, with increased risk to children (Grineski et al., 2011). El Paso residents should be particularly aware of limiting their exposure, especially children's exposure, to the high particulate matter concentrations prevailing in the city during dusty and sandy conditions.

This study has provided important initial data on bulk aeolian deposition in El Paso, Texas, but much more research is needed on this topic. Windblown dust and sand deposition and its characteristics should be measured in other dust-prone regions and cities of North America, such as in the Columbia Plateau and central Great Plains, as well as emerging dust hotspots such as the Salton Sea Basin, to further contextualize deposition rates and physical and chemical properties at the continental scale. Analyses of aeolian deposition samples in El Paso have already shown that windstorms are a method of dispersal of rotifers, nematodes, tardigrades, crustaceans (Rivas et al., 2019), algae and fungi (Rivas et al., 2018); additional analyses could examine which other biota

are dispersed with windblown sand and dust in El Paso and other localities. The presence of microplastics in dry deposition (e.g., Wright et al., 2020) is a rising topic of concern: samples in El Paso and other cities should be carefully analyzed for microplastic distribution. Full annual deposition data are needed, including wet deposition and dry deposition during convective storms and "background" (non-windy) periods. More detailed data on the elemental (trace elements, rare earth elements) and chemical (quantitative XRD, clay mineralogy, organic components, etc.) composition of bulk windblown sediment deposition are also needed. Monitoring fallout of dust and sand at different heights above the ground and different locations both within and outside the urban area in dust-prone dryland cities such as El Paso could clarify the amounts and properties of deposited dust and sand emanating from natural desert sources vs. those contributed by fugitive emissions within urban areas. Additional sampling within the metropolitan area would also improve our understanding of aeolian deposition flux relationships to land use and topography, as well as potential differential impacts on different communities and neighborhoods. Finally, correlating event-by-event deposition and its physical and chemical characteristics to trajectories and weather variables (wind speed, wind gust, moisture) would improve our understanding of meteorological impacts on dust and sand deposition.

Conflict of Interest Statement

None of the authors of the manuscript have any conflicts of interest to report.

Data Availability

Amounts of dust deposited and PM_{10} data for events are available in the Supplementary Data files of Rivas et al. (2019). Some supporting data (HYSPLIT back trajectories for 13 events and laser

diffraction particle size data for 10 events) are available at datarepo.bioinformatics.utep.edu/getdata?acc=ACIEJDV41U1ZN5I . National Weather Service Area Forecast Discussions are available from the Iowa Environmental Mesonet https://mesonet.agron.iastate.edu/wx/afos/list.phtml. PM_{10} and $PM_{2.5}$ data for the CAMS-12 site are available at tceq.texas.gov/cgi-bin/compliance/monops/site_photo.pl?cams=12 . Other data are available upon reasonable request.

Author contributions: CRediT

Conceptualization, TG and EW: Data curation, JR: Formal analysis, TG and JR: Funding acquisition, TG and EW; Investigation, JR, TG, and EW; Methodology, TG; Project administration, TG and EW; Resources, TG and EW; Supervision, TG and EW; Visualization, JR, TG, and EW; Writing- original draft, JR; Writing- review and editing, TG, EW, and JR.

Acknowledgements

Karin Ardon-Dryer, Tristan Chavez-Poeschel, Lixin Jin, Michael Lyubchenko, Syprose Nyachoti, Amanda Ostwald, Patrick Rea, Alison Segura and Eahsan Shahriary are acknowledged for technical assistance. Funding was provided by NSF (DEB 1257068 and 1257116, EW), NIH (5G12RR008124 and 2G12MD007592, EW), NOAA (Office of Education Educational Partnership Program cooperative agreements NA11SEC4810003, NA16SEC4810006 and NA22SEC4810015, TG), and UTEP's Interdisciplinary Research Program (EW and TG). We acknowledge the NOAA Air Resources Laboratory (ARL) for the provision of the HYSPLIT transport and dispersion model and/or READY website (http://www.ready.noaa.gov) used in this work.

References Cited

Abuzaid, H., Awad, M., Shamayleh, A., 2022. Impact of dust accumulation on photovoltaic panels: a review paper. Intl. J. Sustainable Engr. 15(1), 264-285.

Aciego, S. M., Riebe, C. S., Hart, S. C., Blakowski, M. A., Carey, C. J., Aarons, S. M., Dove, N. C., Botthoff, J. K., Sims, K. W. W., Aronson, E. L., 2017. Dust outpaces bedrock in nutrient supply to montane forest ecosystems. Nature Commun. 8(1), 14800.

Al-Abadleh, H. A., Kubicki, J. D., Meskhidze, N., 2023. A perspective on iron (Fe) in the atmosphere: air quality, climate, and the ocean. Environmental Sci. Proc. Impacts 25(2), 151-164.

Al-Awadhi, J. M., Al-Shuaibi, A. A., 2013. Dust fallout in Kuwait City: deposition and characterization. Sci. Total Environ. 461, 139-148.

Ardon-Dryer, K., Kelley, M. C., Xueting, X., Dryer, Y., 2022. The Aerosol Research Observation Station (AEROS). Atmos. Meas. Tech. 15, 2345–2360, https://doi.org/10.5194/amt-15-2345-2022

Ardon-Dryer, K., Gill, T. E., Tong, D. Q., 2023. When a dust storm is not a dust storm: Reliability of dust records from the Storm Events Database and implications for geohealth applications. GeoHealth 7, e2022GH000699, https://doi.org/10.1029/2022GH000699

Baddock, M. C., Gill, T. E., Bullard, J. E. Dominguez Acosta, M., Rivera Rivera, N. I., 2011. Geomorphology of the Chihuahuan Desert based on potential dust emissions. J. Maps 7, 249-259.

Baddock, M. C., Ginoux, P., Bullard, J. E., Gill, T. E., 2016. Do MODIS-defined dust sources have a geomorphological signature? Geophys. Res. Lett. 43, 2606-2613.

Baddock, M. C., Bryant, R. G., Dominguez Acosta, M., Gill, T. E., 2021. Understanding dust sources through remote sensing: Making a case for CubeSats. J. Arid Environ. 184, 104335.

Belnap, J., Reynolds, R. L., Reheis, M. C., Phillips, S. L., Urban, F. E., Goldstein, H. L., 2009. Sediment losses and gains across a gradient of livestock grazing and plant invasion in a cool, semi-arid grassland, Colorado Plateau, USA. Aeolian Res. 1(1-2), 27-43.

Bestelmeyer, B. T., Williamson, J. C., Talbot, C. J., Cates, G. W., Duniway, M. C., Brown, J. R., 2016. Improving the Effectiveness of Ecological Site Descriptions: General State-and-Transition Models and the Ecosystem Dynamics Interpretive Tool (EDIT). Rangelands 38(6), 329- 335, https://doi.org/10.1016/j.rala.2016.10.001.

Blakowski, M. A., Putman, A. L., Jones, D. K., DiViesti, D. N., Hynek, S. A., Fernandez, D. P., Mendoza, D., 2022. Dust and sediment data from Great Salt Lake and the Wasatch Front, Utah, 2018-19. U.S. Geological Survey data release. https://doi.org/10.5066/P996NOES.

Blakowski, M. A., Putman, A. L., DiViesti, D. N., Fernandez, D. P., Jones, D. K., McDonnell, M. C., 2023. Dust and sediment data from Great Salt Lake and northern Utah, 2022. U.S. Geological Survey data release. https://doi.org/10.5066/P9YF6Z4E.

Brahney, J.. 2019. Estimating Total and Bioavailable Nutrient Loading to Utah Lake from the Atmosphere. Utah State University, Watershed Sciences Faculty Publications. Paper 1094. https://doi.org/10.15142/em0e-tt24

Cahill, T. A., Gill, T. E., Reid, J. S., Gearhart, E. A., Gillette, D. A., 1996. Saltating particles, playa crusts and dust aerosols at Owens (dry) Lake, California. Earth Surf. Proc. Landforms 21(7), 621-639.

Capo, R. C., Chadwick, O. A., 1999. Sources of strontium and calcium in desert soil and calcrete. Earth Planetary Sci. Lett. 170, 61- 72.

Castiglia, P. J., Fawcett, P. J., 2006. Large Holocene lakes and climate change in the Chihuahuan Desert. Geology 34, 113-116.

Crabtree, G. W., 2004. Dustfall on the southern high plains of Texas. M.S. thesis, Texas Tech University. http://hdl.handle.net/2346/1225.

Dayalu, A., Calkins, C., Hegarty, J., Alvarado, M., 2024. PM2.5 anomaly detection for exceptional event demonstrations: A Texas case study. J. Air Waste Manage. 74, 771-782, doi:10.1080/10962247.2024.2401368

Dominguez Acosta, M., Gill, T. E., 2007. PIXE based geochemical characterization of the pluvial Lake Palomas system, Chihuahua, Mexico. Proceedings of the 11th International Conference on PIXE and its Analytical Applications, Puebla, Mexico, May 2007, ISBN 978-970-32-5115-5, UNAM Press, Mexico D.F., paper PII-33.

Dominguez Acosta, M., Gill, T. E., Peinado, P., 2010. Geochemical characterization of an aeolian corridor in Northern Chihuahua, Mexico. Actas del INAGEQ (Instituto Nacional de Geoquímica, Mexico) 16, 198- 209.

Duniway, M. C., Pfennigwerth, A. A., Fick, S. E., Nauman, T. W., Belnap, J., Barger, N. N., 2019. Wind erosion and dust from US drylands: a review of causes, consequences, and solutions in a changing world. Ecosphere 10(3), e02650. doi:10.1002/ecs2.2650.

Eagar, J. D., Herckes, P., Hartnett, H. E., 2017. The characterization of haboobs and the deposition of dust in Tempe, AZ from 2005 to 2014. Aeolian Res. 24, 81-91.

Eibedingil, I. G., Gill, T. E., Kandakji, T., Lee, J. A., Li, J., Van Pelt, R. S., 2024. Effect of spatial and temporal “drought legacy” on dust sources in adjacent ecoregions. Land Degrad. Dev. 35(4), 1511-1525.

Erell, E., Tsoar, H., 1997. An experimental evaluation of strategies for reducing airborne dust in desert cities. Build. Environ. 32(3), 225-236.

Feldman, C., 1983. Behavior of Trace Refractory Minerals in the Lithium Metaborate Fusion-Acid Dissolution Procedure. Anal. Chem. 55, 2451-2453.

Fryberger, S., Ahlbrandt, T., Andrews, S., 1979. Origin, sedimentary features, and significance of low-angle eolian sand sheet deposits, Great Sand Dunes National Monument and vicinity, Colorado. J. Sed. Petrol. 49(3), 733-46.

Garcıa, J. H., Li W. W., Arimoto, R., Okrasinski, J. Greenlee, J., Walton, J., Schloesslin, C., Sage, S. 2003. Characterization and implication of potential fugitive dust sources in the Paso del Norte region. Sci. Total Environ. 325, 95–112.

García, J. H., Li, W. W., Cárdenas, N., Arimoto, R., Walton, J., Trujillo, D. 2006. Determination of $PM_{2.5}$ sources using time-resolved integrated source and receptor models. Chemosphere 65(11), 2018-2027.

Gile, L. H., Grossman, R. B. 1979. The desert project soil monograph: Soils and landscapes of a desert region astride the Rio Grande Valley near Las Cruces, New Mexico. US Department of Agriculture, Soil Conservation Service.

Gile, L. H., Hawley, J.W., Grossman, R. B. 1981. Soils and geomorphology in the Basin and Range area of southern New Mexico: Guidebook to the Desert Project, New Mexico. New Bureau of Mines and Mineral Resources Memoir 39, 222 pp.

Gill, T. E., Reynolds, R. L., Zobeck, T. M. 2000. Measurements of current and historic settled dusts in west Texas. Proceedings of the 93rd Air and Waste Management Association Annual Conference and Exhibition, Salt Lake City, Utah, paper 0175.

Gill, T. E., Stout, J. E., Peinado, P. 2009. Composition and characteristics of aerosols in the Southern High Plains of Texas (USA). AIP Conf. Proc. 1099, 255-258.

Gillette, D., Monger, H. C., 2006. Eolian Processes in the Jornada Basin. In: Havstad, K., Huenneke, L. F., Schlesinger, W. H. (Eds.) Structure and Function of Chihuahuan Desert Ecosystem; The Jornada Basin Long-Term Ecological Research Site. New York: Oxford University Press, pp. 189-210.

Gong, K., Zhang, J., Huang, N., Shao, Y., Li, X., 2024. A numerical study on the collection efficiency of devices for atmospheric dust deposition. Catena 236, 107736.

Goodman, M. M., Carling, G. T., Fernandez, D. P., Rey, K. A., Hale, C. A., Bickmore, B. R., Nelson, S. T., Munroe, J. S., 2019. Trace element chemistry of atmospheric deposition along the Wasatch Front (Utah, USA) reflects regional playa dust and local urban aerosols. Chem. Geol. 530, 119317.

Goossens, D., 2007. Bias in grain size distribution of deposited atmospheric dust due to the collection of particles in sediment catchers. Catena 70(1), 16-24.

Goossens, D., Offer, Z. Y., 2000. Wind tunnel and field calibration of six aeolian dust samplers. Atmos. Environ. 34(7), 1043-1057.

Goossens, D., Rajot, J. L., 2008. Techniques to measure the dry aeolian deposition of dust in arid and semi-arid landscapes: a comparative study in West Niger. Earth Surf. Proc. Landforms 33, 178-195.

Gorris, M. E., Ardon-Dryer, K., Campuzano, A., Castañón-Olivares, L. R., Gill, T. E., Greene, A., Hung, C. Y., Kaufeld, K. A., Lacy, M., Sánchez-Paredes, E., 2023. Advocating for coccidioidomycosis to be a reportable disease nationwide in the United States and encouraging disease surveillance across North and South America. J. Fungi 9, 83.

Grineski, S. E., Collins, T. W., 2010. Environmental injustices in transnational context: Urbanization and industrial hazards in El Paso/Ciudad Juárez. Environ. Planning A 42(6), 1308-1327.

Grineski, S. E., Staniswalis, J. G., Bulathsinhala, P., Peng, Y., Gill, T. E., 2011. Hospital admissions for asthma and acute bronchitis in El Paso, Texas: Do age, sex, and insurance status modify the effects of dust and low wind events? Environ. Res. 111, 1148-1155.

Haller, L., Claiborn, C., Larson, T., Koenig, J., Norris, G., Edgar, R., 1999. Airborne Particulate Matter Size Distributions in an Arid Urban Area. J. Air Waste Manage. 49(2), 161-168, doi: 10.1080/10473289.1999.10463788

Hand, J. L., Gill, T. E., Schichtel, B. A., 2019. Urban and rural coarse aerosol mass across the United States: Spatial and seasonal variability and long-term trends. Atmos. Environ. 218, 117025.

Herrera-Molina, E., Gill, T. E., Ibarra-Mejia, G., Jeon, S., 2021. Associations between dust exposure and hospitalizations in El Paso, Texas, USA. Atmosphere 12(11), 1413.

Hoerling, M., Eischeid, J., Kumar, A., Leung, R., Mariotti, A., Mo, K., Schubert, S., Seager, R., 2014. Causes and predictability of the 2012 Great Plains drought. Bull. Amer. Meteorol. Soc. 95(2), 269-282.

Huang, M., Tong, D., Lee, P., Pan, L., Tang, Y., Stajner, I., Pierce, R. B., McQueen, J., Wang, J., 2015. Toward enhanced capability for detecting and predicting dust events in the western United States: the Arizona case study. Atmos. Chem. Phys. 15(21), 12595-12610.

Ingasmells, C. O., 1970. Lithium Metaborate Flux in Silicate Analysis. Anal. Chim. Acta 52, 323-334.

Instituto Nacional de Estadística, Geografía e Informática (Mexico), n.d. Carta Edafológica escala 1:250 000 serie I, Ciudad Juárez.

International Union of Soil Sciences Working Group WRB, 2022. World Reference Base for Soil Resources- International soil classification system for naming soils and creating legends for soil maps. 4th edition. International Union of Soil Sciences (IUSS), Vienna, Austria.

Jiao, L., Wang, X., Li, D., 2018. Spatial variation in the flux of atmospheric deposition and its ecological effects in arid Asia. Aeolian Res. 32, 71-91.

Kandakji, T., Gill, T. E., Lee, J. A., 2020. Identifying and characterizing dust point sources in the southwestern United States using remote sensing and GIS. Geomorphology 353, 107019.

Karle, N. N., Fitzgerald, R. M., Sakai, R. K., Sullivan, D. W., Stockwell, W. R., 2021. Multi-scale atmospheric emissions, circulation and meteorological drivers of ozone episodes in El Paso-Juárez airshed. Atmosphere 12(12), 1575.

Kavouras, I. G., DuBois, D. W., Nikolich, G., Avittia, A. C., Etyemezian, V., 2016. Particulate dust emission factors from unpaved roads in the US–Mexico border semi-arid region. J. Arid Environ. 124, 189-192.

Langford, R. P., 2000. Nabkha (coppice dune) fields of south-central New Mexico, USA. J. Arid Environ. 46, 25–41.

Lawrence, C. R., Neff, J. C., 2009. The contemporary physical and chemical flux of aeolian dust: A synthesis of direct measurements of dust deposition. Chem. Geol. 267(1-2), 46-63.

Lee, J. A., Gill, T. E., Mulligan, K. R., Dominguez Acosta, M., Perez, A. E., 2009. Land use/land cover and point sources of the 15 December 2003 dust storm in southwestern North America. Geomorphology 105, 18-27.

Ley, R. E., Williams, M. W., Schmidt, S. K. 2004. Microbial population dynamics in an extreme environment: controlling factors in talus soils at 3750m. Biogeochemistry 68, 313–335.

Li, R., Wiedinmyer, C., Hannigan, M. P., 2013. Contrast and correlations between coarse and fine particulate matter in the United States. Sci. Total Environ. 456, 346-358.

Li, J., Kandakji, T., Lee, J. A., Tatarko, J., Blackwell, J. III., Gill, T. E., Collins, J. D., 2018. Blowing dust and highway safety in the southwestern United States: Characteristics of dust emission “hotspots” and management implications. Sci. Total Environ. 621, 1023-1032.

Lucke, B., Sandler, A., Vanselow, K. A., Bruins, H. J., Abu-Jaber, N., Bäumler, R., Porat, N., Kouki, P., 2019. Composition of modern dust and Holocene Aeolian sediments in archaeological structures of the Southern Levant. Atmosphere 10(12), 762.

Maliszewski, P.J., Larson, E.K., Perrings, C., 2012. Environmental determinants of unscheduled residential outages in the electrical power distribution of Phoenix, Arizona. Reliab. Eng. Syst. Saf. 99, 161-171.

McCoy, B. J., Fischbeck, P. S., Gerard, D., 2010. How big is big? How often is often? Characterizing Texas petroleum refining upset air emissions. Atmos. Environ. 44(34), 4230-4239.

Medlin, J. H., Suhr, N. H., Bodkin, J. B., 1969. Atomic Absorption Analysis of Silicates Employing LiBO2 Fusion. At. Absorpt. News. 8, 25-29.

Mockford, T., Bullard, J. E., Thorsteinsson, T., 2018. The dynamic effects of sediment availability on the relationship between wind speed and dust concentration. Earth Surf. Proc. Landforms 43(11), 2484-2492.

Modaihsh, A., Ghoneim, A., Al-Barakah, F., Mahjoub, M., Nadeem, M., 2017. Characterizations of Deposited Dust Fallout in Riyadh City, Saudi Arabia. Pol. J. Environ. Stud. 26(4), 1599- 1605.

Mukherjee, A., Agrawal, M., 2017. World air particulate matter: sources, distribution and health effects. Environ. Chem. Lett. 15, 283–309.

Munroe, J. S., Santis, A. A., Soderstrom, E. J., Tappa, M. J., Bauer, A. M., 2024. Mineral dust and pedogenesis in the alpine critical zone. Soil 10, 167–187, https://doi.org/10.5194/soil-10-167-2024 .

Munson, S. M., Belnap, J., Okin, G. S., 2011. Responses of wind erosion to climate-induced vegetation changes on the Colorado Plateau. Proc. Nat. Acad. Sci. 108(10), 3854-3859, http://dx.doi.org/10.1073/pnas.1014947108 .

Nakase, D. K., Hartshorn, A. S., Spielmann, K. A., Hall, S. J. (2014). Eolian deposition and soil fertility in a prehistoric agricultural complex in central Arizona, USA. Geoarchaeology 29(2), 79-97.

Novlan, D. J., Hardiman, M., Gill, T. E., 2007. A synoptic climatology of blowing dust events in El Paso, Texas from 1932–2005. Preprints, 16th Conference on Applied Climatology, American Meteorological Society J3.12, 1–13.

Nyachoti, S., Jin, L., Tweedie, C., Ma, L., 2019. Insight into factors controlling formation rates of pedogenic carbonates: A combined geochemical and isotopic approach in dryland soils of the US Southwest. Chem. Geol. 527, 118503, https://doi.org/10.1016/j.chemgeo.2017.10.014

Ono, D. M., Hardebeck, E., Parker, J., Cox, B. G., 2000. Systematic Biases in Measured PM10 Values with U.S. Environmental Protection Agency-Approved Samplers at Owens Lake, California. J. Air Waste Manage. 50, 1144-1156.

Pan, J., Zhao, H., Wang, Y., Liu, G., 2021. The influence of aeolian sand on the anti-skid characteristics of asphalt pavement. Materials, 14, 5523, https://doi.org/10.3390/ma14195523.

Park, S. H., Gong, S. L., Zhao, T. L., Vet, R. J., Bouchet, V. S., Gong, W., Makar, P. A., Moran, M. D., Stroud, C., Zhang, J., 2007. Simulation of entrainment and transport of dust particles within

North America in April 2001 (“Red Dust Episode”). J. Geophys. Res. Atmos. 112(D20), D20209, doi:10.1029/2007JD008443.

Peinado, P., Gill, T. E., Lee, J. A., Dominguez Acosta, M., 2014. Geochemical and physical properties of dust source sediments in the Chihuahuan Desert and Southern High Plains. Geol. Soc. Amer. Ann. Mtg. Abstract 247308.

Perez, A. E., Gill, T. E., 2009. Salt Flat Basin's contribution to regional dust production and potential influence on dry deposition in the Guadalupe Mountains (Texas, USA). Natural Resources and Environmental Issues 15, 117–118.

Péwé, T. L., Péwé, E. A., Péwé, R. H., Journaux, A., Slatt, R. M., 1981. Desert dust: Characteristics and rates of deposition in central Arizona. Geol. Soc. Amer. Spec. Pap. 186, 169-190.

Prakash, P. J., Stenchikov, G., Tao, W., Yapici, T., Warsama, B., Engelbrecht, J. P., 2016. Arabian Red Sea coastal soils as potential mineral dust sources. Atmos. Chem. Phys. 16, 11991-12004.

Prospero, J. M., Ginoux, P., Torres, O., Nicholson, S. E., Gill, T. E., 2002. Environmental characterization of global sources of atmospheric soil dust identified with the Nimbus 7 Total Ozone Mapping Spectrometer (TOMS) absorbing aerosol product. Rev. Geophys. 40, 1002.

Putman, A. L., Jones, D. K., Blakowski, M. A., DiViesti, D., Hynek, S. A., Fernandez, D. P., Mendoza, D., 2022. Industrial particulate pollution and historical land use contribute metals of concern to dust deposited in neighborhoods along the Wasatch Front, UT, USA. GeoHealth, 6(11), e2022GH000671.

Putman, A. L., Blakowski, M. B., McDonnell, M., DiViesti, D., Fernandez, D., Longley, P., Jones, D. K., 2023. Assessing exposure of northern Utah communities to dust from the contaminated and dynamic Great Salt Lake playa. Report prepared by the U.S. Geological Survey for the Utah Department of Natural Resources, Division of Forestry Fire and State Lands.

Rashki, A., Eriksson, P. G., Rautenbach, C. D. W., Kaskaoutis, D. G., Grote, W., Dykstra J., 2013. Assessment of chemical and mineralogical characteristics of airborne dust in the Sistan region, Iran. Chemosphere 90, 227–236.

Raysoni, A. U., Sarnat, J. A., Sarnat, S. E., Garcia, J. H., Holguin, F., Luèvano, S. F., Li, W. W., 2011. Binational school-based monitoring of traffic-related air pollutants in El Paso, Texas (USA) and Ciudad Juárez, Chihuahua (México). Environ. Pollut. 159(10), 2476-2486.

Rea, P., Ma, L., Gill, T. E., Gardea-Torresdey, J., Tamez, C., Jin, L., 2020. Tracing gypsiferous White Sands aerosols in the shallow critical zone in the northern Sacramento Mountains, New Mexico using Sr/Ca and 87Sr/86Sr ratios. Geoderma 372, 114387.

Reheis, M. C., 2003. Dust Deposition in Nevada, California, and Utah, 1984-2002. U.S. Geol. Surv. Open-File Rep. 03-138.

Reheis, M. C., Kihl, R., 1995. Dust deposition in southern Nevada and California, 1984– 1989: relations to climate, source area, and source lithology. J. Geophys. Res. 100 (D5), 8893–8918.

Reheis, M. C., Urban, F. E., 2011. Regional and climatic controls on seasonal dust deposition in the southwestern US. Aeolian Res. 3(1), 3-21.

Reheis, M. C., Goodmacher, J. C., Harden, J. W., McFadden, L. D., Rockwell, T. K., Shroba, R. R., Sowers, J. M., Taylor, E. M., 1995. Quaternary soils and dust deposition in southern Nevada and California. Geol. Soc. Am. Bull. 107(9), 1003-1022.

Reheis, M. C., Budahn, J. E., Lamothe, P. J., Reynolds, R. L., 2009. Compositions of modern dust and surface sediments in the Desert Southwest, United States. J. Geophys. Res., 114, F01028, doi:10.1029/2008JF001009

Reynolds, R. L., Goldstein, H. L., Moskowitz, B. M., Bryant, A. C., Skiles, S. M., Kokaly, R. F., Flagg, C. B., Yauk, K., Berquó, T., Breit, G., Ketterer, M., 2014. Composition of dust deposited to snow cover in the Wasatch Range (Utah, USA): Controls on radiative properties of snow cover and comparison to some dust-source sediments. Aeolian Res. 15, 73-90.

Reynolds, R. L., Goldstein, H. L., Moskowitz, B. M., Kokaly, R. F., Munson, S. M., Solheid, P., Breit, G. N., Lawrence, C. R., Derry, J., 2020. Dust deposited on snow cover in the San Juan Mountains, Colorado, 2011–2016: Compositional variability bearing on snow-melt effects. J. Geophys. Res. Atmos. 125, e2019JD032210. https://doi.org/10.1029/2019JD032210

Rivas Jr., J. A., 2019. Dust storms and the dispersal of aquatic microinvertebrates in the Chihuahuan Desert ecoregion. Dissertation, University of Texas at El Paso.

Rivas Jr., J. A., Mohl, J. E., Van Pelt, R. S., Leung, M. Y., Wallace, R. L., Gill, T. E., Walsh, E. J., 2018. Evidence for regional aeolian transport of freshwater micrometazoans in arid regions. Limnol. Oceanog. Lett. 3, 320–330.

Rivas Jr., J.A., Schröder, T., Gill, T. E., Wallace, R. L., Walsh, E. J., 2019. Anemochory of diapausing stages of microinvertebrates in North American drylands. Freshwater Biol. 64, 1303-1314. https://doi.org/10.1111/fwb.13306

Rivera Rivera, N.I., 2012. Analysis And Modeling Of Dust Event Data From El Paso, Texas. Dissertation, University of Texas at El Paso.

Rivera Rivera, N.I., Gill, T. E., Gebhart, K. A., Hand, J. L., Bleiweiss, M. P., Fitzgerald, R. M., 2009. Wind modelling of Chihuahuan Desert outbreaks. Atmos. Environ. 43, 347-354.

Rivera Rivera, N. I., Gill, T. E., Bleiweiss, M. P., Hand, J. L., 2010. Source characteristics of hazardous Chihuahuan Desert dust outbreaks. Atmos. Environ. 44, 2457–2468.

Robinson, M. C., Ardon-Dryer, K., 2024. Characterization of 21 years of dust events across four West Texas regions. Aeolian Res. 67, 100930.

Ruppecht, E., Meyer, M., Patashnick, H., 1992. The tapered element oscillating microbalance as a tool for measuring ambient particulate concentrations in real time. J. Aerosol Sci. 23 (Supp. 1), 635-638.

Sánchez, A. S., Cohim, E., Kalid, R. A., 2015. A review on physicochemical and microbiological contamination of roof-harvested rainwater in urban areas. Sustain. Water Qual. Ecol. 6, 119-137.

SAS Institute Inc. 2019. Base SAS® 9.4 Procedures Guide. Cary, NC: SAS Institute Inc.

Scholz, J., Brahney, J. 2019. Evaluating catchment and atmospheric drivers for phosphorus increases in mountain lakes of Northeastern Utah. Poster presented at Society for Freshwater Science, Salt Lake City, Utah, May 19-23, 2019.

Shao, Y. 2008. Physics and modelling of wind erosion. Springer, Dordrecht.

Sharratt, B., Pi, H., 2018. Field and laboratory comparison of PM10 instruments in high winds. Aeolian Res. 32, 42-52.

Soheili, F., Woodward, S., Abdul-Hamid, H., Naji, H. R., 2023. The effect of dust deposition on the morphology and physiology of tree foliage. Water Air Soil Poll. 234(6), 339.

Soil Survey Division Staff, 1993. Soil survey manual. Soil Conservation Service, U.S. Department of Agriculture Handbook 18, Chapter 3.

Soil Survey Staff, Natural Resources Conservation Service, United States Department of Agriculture, 2024. Web Soil Survey. Online at http://websoilsurvey.sc.egov.usda.gov/. Accessed November 26, 2024.

Sorooshian, A., Wonaschütz, A., Jarjour, E. G., Hashimoto, B. I., Schichtel, B. A., Betterton, E. A., 2011. An aerosol climatology for a rapidly growing arid region (southern Arizona): Major aerosol species and remotely sensed aerosol properties. J. Geophys. Res. Atmos. 116(D19), D19205, doi:10.1029/2011JD016197.

Sow, M., Goossens, D., Rajot, J. L., 2006. Calibration of the MDCO dust collector and of four versions of the inverted frisbee dust deposition sampler. Geomorphology 82, 360–375.

Sperazza, M., Moore, J. N., Hendrix, M. S., 2004. High-resolution particle size analysis of naturally occurring very fine-grained sediment through laser diffractometry. J. Sediment. Res. 74, 736–743.

Stein, A. F., Draxler, R. R., Rolph, G. D., Stunder, B. J. B., Cohen, M. D., Ngan, F., 2015. NOAA's HYSPLIT atmospheric transport and dispersion modeling system. Bull. Amer. Met. Soc. 96, 2059–2077.

Stout, J. E., 2001. Dust and environment in the southern high plains of North America. J. Arid Environ. 47, 425-441.

Suhr, N. H., Ingasmells, C. O., 1966. Solution Technique for Analysis of Silicates. Anal. Chem. 38, 730-734.

Tong, D. Q., Wang, J. X., Gill, T. E., Lei, H., Wang, B., 2017. Intensified dust storm activity and Valley fever infection in the southwestern United States. Geophys. Res. Lett. 44, 4304-4312.

Tong, D. Q., Gill, T. E., Sprigg, W. A., Van Pelt, R. S., Baklanov, A. A., Barker, B. M., Bell, J. E., Castillo, J., Gassó, S., Gaston, C. J., Griffin, D. W., Huneeus, N., Kahn, R. A., Kuciauskas, A. P., Ladino, L. A., Li, J., Mayol-Bracero, O. L., McCotter, O. Z., Méndez-Lázaro, P. A., Mudu, P., Nickovic, S., Oyarzun, D., Prospero, J., Raga, G. P., Raysoni, A. U., Ren, N., Sarafoglou, N., Sealy, A., Sun, Z., Vukovic Vimic, A., 2023. Health and safety effects of airborne soil dust in the Americas and beyond. Rev. Geophys. 61, e2021RG000763. https://doi.org/10.1029/2021RG000763

Velarde, R., 2011. Evaluating suspended dust particulate matter from anthropogenically-altered lands. Dissertation, University of Texas at El Paso.

Wan, D., Jin, Z., Wang, Y., 2012. Geochemistry of eolian dust and its elemental contribution to Lake Qinghai sediment. Appl. Geochem. 27(8), 1546-1555.

Warn, G. F., Cox, W. H., 1951. A sedimentary study of dust storms in the vicinity of Lubbock, Texas. Amer. J. Sci. 249, 553-568.

White, W. H., Hyslop, N. P., Trzepla, K., Yatkin, S., Rarig, R. S. Jr., Gill, T. E., Jin, L., 2015. 2015. Regional transport of a chemically distinctive dust: Gypsum from White Sands, New Mexico (USA). Aeolian Res. 16, 1-10.

Wright, S. L., Ulke, J., Font, A., Chan, K. L. A., Kelly, F. J., 2020. Atmospheric microplastic deposition in an urban environment and an evaluation of transport. Environ. Intl. 136, 105411, doi:10.1016/j.envint.2019.105411

Yan, Y., Chen, H., Liang, L., Ma, L., Liu, X., Liu, H., Sun, Y., 2017. Meteorological constraints on characteristics of daily dustfall in Xi'an. Atmos. Environ. 158, 98-104.

Zar, J. 2009. Biostatistical analysis (5th edition). Pearson, London.

Zhang, L., Gong, S., Padro, J., Barrie, L., 2001. A size-segregated particle dry deposition scheme for an atmospheric aerosol module. Atmos. Environ. 35(3), 549–560. https://doi.org/10.1016/S1352-2310(00)00326-5

Zhang, P., Sherman, D. J., Li, B., 2021. Aeolian creep transport: A review. Aeolian Res. 51, 100711.